Regulation and Localization of the Bloom Syndrome Protein in Response to DNA Damage

Oliver Bischof,* Sahn-Ho Kim,* John Irving,‡ Sergey Beresten,§ Nathan A. Ellis,§ and Judith Campisi*

*Life Sciences Division, Lawrence Berkeley National Laboratory, Berkeley, California 94720; ‡Berlex Laboratories, Inc., Richmond, California 94804; and §Department of Human Genetics, Memorial Sloan-Kettering Cancer Center, New York, New York 10021

Abstract. Bloom syndrome (BS) is an autosomal recessive disorder characterized by a high incidence of cancer and genomic instability. BLM, the protein defective in BS, is a RecQ-like helicase, presumed to function in DNA replication, recombination, or repair. BLM localizes to promyelocytic leukemia protein (PML) nuclear bodies and is expressed during late S and G2. We show, in normal human cells, that the recombination/repair proteins hRAD51 and replication protein (RP)-A assembled with BLM into a fraction of PML bodies during late S/G2. Biochemical experiments suggested that BLM resides in a nuclear matrix–bound complex in which association with hRAD51 may be direct. DNA-damaging agents that cause double strand breaks and a G2 delay induced BLM by a p53- and ataxia-telangiectasia mutated independent mechanism. This induction depended on the G2 delay, because it failed to occur when G2 was prevented or bypassed. It coincided with the appearance of foci containing BLM, PML, hRAD51 and RP-A, which resembled ionizing radiation-induced foci. After radiation, foci containing BLM and PML formed at sites of single-stranded DNA and presumptive repair in normal cells, but not in cells with defective PML. Our findings suggest that BLM is part of a dynamic nuclear matrix–based complex that requires PML and functions during G2 in undamaged cells and recombinational repair after DNA damage.

Key words: RECQ helicases • p53 • ATM • nuclear matrix • homologous recombination

Introduction

Several genes have evolved to ensure the integrity and stability of cellular genomes. Some of these genes are conserved from bacteria to humans, whereas others are restricted to eukaryotes or mammals. In mammals, failure to maintain genomic stability almost inevitably leads to cancer. At present, we have only a rudimentary understanding of the pathways by which genomic stability is maintained in mammalian cells, particularly human cells.

Recent findings implicate genes related to *Escherichia coli RECQ* in maintaining genomic stability in human cells. *RECQ* encodes a DNA helicase that acts in homologous recombination (HR)[1] and suppresses illegitimate recombination, particularly during the repair of DNA double strand breaks (DSBs; Hanada et al., 1997; Harmon and Kowalczykowski, 1998). *RECQ*-like genes are prevalent throughout evolution. Budding and fission yeast have a single gene (SGS1, RQH1/RAD12), which participates in recombination and chromosome segregation (Stewart et al., 1997; Watt et al., 1997; Davey et al., 1998). Mammalian cells require *RECQ*-like functions to maintain genomic integrity, but, in contrast to *E. coli* and yeast, have multiple *RECQ*-like genes. Five human *RECQ*-like genes have been identified: *RECQL* (alias *RecQ1*), *BLM*, *WRN*, *RECQL4* (alias *RecQ4*), and *RECQL5* (alias *RecQ5*) (Puranam and Blackshear, 1994; Seki et al., 1994; Ellis et al., 1995; Yu et al., 1996; Kitao et al., 1998). Each contains a region with strong homology to seven motifs that specify the *RECQ* helicase activity. Indeed, biochemical assays showed that RECQL, BLM, and WRN encode proteins that are 3′–5′ DNA helicases (Tada et al., 1996; Gray et al., 1997; Karow et al., 1997). Despite strong homology in the helicase domains, human *RECQ*-like genes differ markedly outside these domains. Moreover, three of these genes are associated with autosomal recessive disorders that, despite some similarities, display striking phenotypic differences.

Address correspondence to Judith Campisi, Lawrence Berkeley National Laboratory, Mailstop 84-171, Berkeley, CA 94720. Tel.: (510) 486-4416. Fax: (510) 486-4545. E-mail: jcampisi@lbl.gov

O. Bischof's present address is Institute Pasteur, 28 rue de Dr. Roux, 75724 Paris, Cedex 15, France.

[1]*Abbreviations used in this paper:* AT, ataxia telangiectasia; ATM, AT mutated; BS, Bloom syndrome; DSB, double-strand break; DNA-PK, DNA-dependent protein kinase; GST, glutathione *S*-transferase; HR, homologous recombination; HU, hydroxyurea; IR, ionizing radiation; IRIF, IR-induced foci; LN, labeled nuclei; NB, nuclear body; PARP, poly-ADP ribose polymerase; PML, promyelocytic leukemia protein; RP, replication protein; RT, reverse transcriptase; RTS, Rothmund-Thomson syndrome; SCE, sister chromatid exchange; WS, Werner syndrome.

The first human *RECQ*-like gene that was linked to a hereditary disorder was *BLM*, the gene defective in Bloom syndrome (BS). Individuals with BS suffer from acute symptoms, including pre- and postnatal growth retardation, immunodeficiency, and male infertility. BS individuals also have a very high incidence of cancer. Cancer is the primary cause of death, which generally occurs before the third decade of life. BS cells are hypermutable, showing numerous chromatid gaps and breaks and many sister chromatid exchanges (SCEs) (German, 1993; Ellis and German, 1996; Watt and Hickson, 1996). Defects in *WRN* and *RECQL4* have also been linked to hereditary disorders: Werner syndrome (WS), in the case of *WRN*, and a subset of Rothmund-Thomson syndrome (RTS), in the case of *RECQL4*. WS and RTS share several features with BS, most notably a high incidence of cancer (Vennos and James, 1995; Watt and Hickson, 1996; Martin et al., 1999). In addition, WS and RTS cells, like BS cells, are hypermutable (Fukuchi et al., 1989; Miozzo et al., 1998). However, there are marked differences. WS individuals are asymptomatic before puberty, but thereafter develop a panoply of age-related disorders, including cardiovascular disease, cataracts, and osteoporosis (Goto, 1997). RTS individuals have distinctive skin and skeletal abnormalities (Starr et al., 1985; Vennos and James, 1995). Moreover, despite being hypermutable, WS and RTS cells do not show the high rate of SCE characteristic of BS cells.

The high incidence of cancer and genomic instability in BS, WS, and RTS suggest that the functions of *BLM*, *WRN*, and *RECQL4* may overlap. On the other hand, the phenotypic differences among BS, WS, and RTS suggest that these genes have distinct functions. By analogy with *RECQ*, human *RECQ*-like genes are presumed to function in DNA replication, recombination, and/or repair. However, little is known about the specific processes in which they participate.

BLM expression, in contrast to that of other human *RECQ*-like genes (Gray et al., 1998; Kitao et al., 1998), is cell cycle regulated, peaking in late S phase and G2 (Gharibyan and Youssoufian, 1999; Dutertre et al., 2000), and localizing to nuclear foci containing the promyelocytic leukemia protein (PML) tumor suppressor (Gharibyan and Youssoufian, 1999; Ishov et al., 1999; Zhong et al., 1999). We show that BLM protein and foci are also induced by agents that cause DNA DSBs. This induction was indirect and due to the G2 delay caused by the agents. BLM foci also contained the recombination/repair proteins hRAD51 and replication protein (RP)-A and BLM was a component of the RAD51 ionizing radiation-induced foci (IRIF), which form in response to ionizing radiation (IR) (Haaf et al., 1995; Maser et al., 1997; Golub et al., 1998). Moreover, both BLM and PML associated with sites of putative repair after IR-induced damage. Our results suggest that BLM is a component of a nuclear matrix–based complex, which resides in the PML bodies and forms increasingly during G2 in undamaged cells and in response to potentially recombinogenic DNA damage.

Materials and Methods

Cell Culture

Proliferative capacity was assessed by labeling cells for 72 h with [^{3}H]thymidine (10 μCi/ml) and autoradiography to determine the percentage of radiolabeled nuclei (% LN) (Dimri et al., 1994, 1995). Human WI-38 fetal lung fibroblasts were used at early passage (>70% LN) or senescence (<10% LN), as indicated. E6-expressing WI-38 (Dimri et al., 2000) cells were generated by retroviral transfer of the human papilloma virus E6 gene (Halbert et al., 1992). E. Blakely and D. Chen (Lawrence Berkeley National Laboratory) provided ataxia telangiectasia (AT)-2SF and MO59J (DNA-PKcs–deficient) cells, respectively; J. German (Cornell Medical School, Ithaca, NY) provided BS fibroblasts HG2654; and O. Pereira-Smith (Baylor College of Medicine, Houston, TX) provided HT1080 and HCA2 cells. VA-13 and SAOS-2 cells, and BS fibroblasts GM001492F were from the American Type Culture Collection. Unless noted otherwise, cells were cultured in Dulbecco's modified Eagle's medium containing 10% fetal bovine serum.

Cell Cycle Measurements

Proliferating cells were made quiescent by culturing in 0.2% serum for 72–96 h and stimulated to proliferate with 10% serum. To block cells at G1/S, quiescent cells were stimulated for 10–12 h, given 5 mM hydroxyurea (HU; Sigma-Aldrich) for 12–16 h in 10% serum, and released by washing and providing drug-free 10% serum (Lu et al., 1989). Entry into and through S phase was monitored by a 1-h pulse with [^{3}H]thymidine and autoradiography, as described above. Cell cycle distributions were assessed by flow cytometry of propidium iodide–stained nuclei (Pucillo et al., 1990) using a FACScan™ and Lysis II software (Becton Dickinson). Mitotic indices were determined by fixing cells in 3:1 methanol/acetic acid, staining with 0.5 mg/ml propidium iodide in PBS, and counting mitotic figures by fluorescence microscopy. 1,000 nuclei were counted for each point.

Irradiation and Drug Treatment

Cells were X-irradiated (1.8 Gy/min) in 10% serum using a PANTAK HF160 generator (Comet Ag), and UV-irradiated (1.6 J/m^2/s) in PBS using a UVC GTE G875 bulb. Bleomycin (10 mg/ml in PBS), etoposide (10 mM in dimethylsulfoxide; Calbiochem), hydrogen peroxide (30%), and caffeine (Sigma-Aldrich) were diluted into 10% serum before use. Cells were given media containing drug or solvent for 1 h at 37°C, unless noted otherwise, washed, and given drug-free 10% serum.

Antibodies

The affinity-purified rabbit anti-BLM antibody has been described (Ishov et al., 1999; Neff et al., 1999; Zhong et al., 1999). It did not detect an ~160-kD band in Western blots of BS cells (not shown). Rabbit anti-hRAD51 IgG was a gift from Dr. D. Chen (Lawrence Berkeley National Laboratory) or purchased from Oncogene Research Products. α-Tubulin (Ab1) and RP-A (Ab1, Ab2) antibodies were from Oncogene Research Products, BrdU antibody was from Boehringer, poly-ADP ribose polymerase (PARP) antibody (H-250) was from Santa Cruz Biotechnology, Inc., anti-Ku70 (clone N3H10) was from NeoMarkers, and fluorescent or horseradish peroxidase–conjugated secondary antibodies were from Vector Laboratories or Bio-Rad Laboratories.

Immunofluorescence

Cells in 4-well glass slides were cultured 2–4 d before irradiation or synchronization, fixed and stained as described (Compton et al., 1991), incubated with primary antibody for 2 h, and secondary (fluorescein isothiocyanate– or Texas red–labeled) antibody for 1 h. BLM and hRAD51 were detected using a Fab fragment secondary antibody (Wessel and McClay, 1986; Jackson ImmunoResearch Laboratories). Slides were mounted in VectaShield containing DAPI (0.4 μg/ml; Vector Laboratories) to visualize nuclear DNA and viewed by epifluorescence or a single laser confocal section. Foci (at least 200 nuclei/data point) were scored at 600× magnification. Images were captured with a CCD camera and merged using Canvas (Deneba).

Detection of Single Strand DNA after Damage

Cells were grown on slides in 10% serum containing 10 μg/ml BrdU for 30 h and X-irradiated in BrdU-free medium as described (Raderschall et al., 1999). Cells were fixed at the indicated times after irradiation (Compton et al., 1991) and immunostained using mouse anti-BrdU IgG and FITC-goat anti–mouse IgG (Boehringer), or rabbit anti-BLM IgG and Texas red goat anti–rabbit IgG. Cells were counterstained with DAPI and viewed as described above.

Western Analysis

Total protein lysates were prepared in 2× SDS-PAGE sample buffer and 30 μg protein was separated by 4–15% SDS-PAGE and analyzed by Western blotting as described (Dimri et al., 1996). Antibodies were detected by chemiluminescence using SuperSignal (PierceChemical Co.). Signals were quantified by densitometry using ImageQuant software (Molecular Dynamics).

TaqMan Reverse Transcriptase PCR Analyses

Total RNA was prepared using a commercial kit (Promega). One-step reverse transcriptase (RT)-PCR was performed using the TaqMan Gold RT-PCR kit (PerkinElmer) according to the manufacturer's instructions. RT-PCR reactions were performed on 40 ng RNA, in triplicate, using an ABI 7700 Sequence Detection system (Heid et al., 1996). Primer and fluorogenic probes used for *BLM* and *QM* were designed using Primer Express software (PerkinElmer). The primer/probe sequences were: forward 5′-CTGATGCCGACTGGAGGTG-3′, reverse 5′-TGACAACAGTGACCCCAGGA-3′, probe 5′FAM-AGTTTGTGTTACCAGCTCCCTGCCTGTGT-3′ for *BLM*; forward 5′-TGCGGCTCCACCCCTT-3′, reverse 5′-GCATGCCTGTTTGGAGCCT-3′, probe 5′FAM-CACGTCATCCGCATCAACAAGATGTTG-3′ for *QM*. Triplicate measurements were averaged and normalized to triplicate measurements of 18 S ribosomal RNA (TaqMan ribosomal RNA control reagent kit) or *QM* (Dimri et al., 1996) mRNA with similar results using 40 pg RNA per reaction. Values reported are normalized to *QM* mRNA.

BLM–hRAD51 Interaction

Glutathione *S*-transferase (GST) and GST-BLM fusion protein were expressed in Sf9 cells infected with recombinant baculoviruses using a commercial kit (GIBCO BRL). Nuclear lysates (Dignam et al., 1983) from infected cells were clarified by centrifugation and incubated for 1 h at 4°C with glutathione-Sepharose 6-CL B resin (Amersham Pharmacia Biotech). The slurry was transferred to a column and washed with 50 column volumes each of PBS plus 0.2% NP-40 and PBS. Nuclear lysates prepared from SAOS-2 cells were pretreated with DNase I (160 U/ml) for 30 min at 37°C, after which ethidium bromide was added to 250 μg/ml. These nuclear lysates were incubated with glutathione-Sepharose to which GST or GST-BLM for 1 h at 4°C. The resin was washed with 50 vol each of PBS plus 0.5% NP-40, PBS plus 0.2% NP-40, and PBS. Proteins were eluted from the resin with 20 mM glutathione, 100 mM Tris, pH 8.0, 150 mM NaCl, 1 mM DTT, and 10% glycerol, and those remaining after elution were released by boiling in 2× SDS-PAGE sample buffer. Eluted proteins and proteins released by boiling (30 μg) were analyzed by 4–15% SDS-PAGE and Western blotting for BLM, hRAD51, poly-ADP-ribose polymerase, and Ku70. For immunoprecipitation, SAOS-2 nuclear lysates were precleared by incubating with 5 μg rabbit IgG and Dynabeads-protein G (Bio-Rad Laboratories) for 1 h at 4°C with gentle agitation. The beads were collected and the supernatant was incubated with 5 μg rabbit anti-RAD51 (Oncogene Research Products) for 16 h at 4°C, followed by addition of Dynabeads for 1 h at 4°C. The beads were collected, washed extensively with PBS plus 0.2% NP-40, and washed once with PBS. Immune complexes were released from the beads by boiling in 2× SDS-PAGE sample buffer, and analyzed by 4–15% SDS-PAGE and Western blotting for BLM and hRAD51.

Nuclear Matrix Preparation

Nuclear matrix was prepared from cells (80% confluent) by either of two methods as described (Wan et al., 1999). In brief, cells were suspended at 5×10^6/ml in 0.3 M sucrose, 3 mM $MgCl_2$, 1 mM EGTA, 10 mM PIPES, pH 6.9, 100 mM NaCl, proteinase inhibitor mix (Boehringer), and 10 U/ml prime RNase inhibitor (Promega) (suspension buffer), permeabilized by addition of 0.5% Triton X-100 for 7 min on ice, and washed in suspension buffer. Nuclei were collected by centrifugation, digested with DNase I (300 U/ml, 37°C, 30 min), pelleted, and extracted by 0.25 M ammonium sulfate followed by 2 M NaCl or two incubations with *N*-hydroxysulfosuccinimide acetate (Pierce Chemical Co.), all in suspension buffer, for 20 min at room temperature. The pellet was digested with RNase A (10 μg/ml in suspension buffer) for 20 min on ice, solubilized by addition of 2% SDS, and analyzed by SDS-PAGE and Western blotting.

Results

BLM Localizes to PML Nuclear Bodies with hRAD51 and RP-A during Late S/G2

BLM is expressed most highly during S phase and G2 and localizes to nuclear foci in a fraction of asynchronously dividing cells (Gharibyan and Youssoufian, 1999; Neff et al., 1999; Dutertre et al., 2000). These foci were identified as PML nuclear bodies (NBs) (Ishov et al., 1999; Zhong et al., 1999). PML is a tumor suppressor that inhibits cell proliferation and promotes apoptosis in many cells (de The et al., 1991; Mu et al., 1994; Le et al., 1996; Wang et al., 1998a,b).

To follow assembly of BLM into PML NBs and identify other components in PML/BLM foci, we monitored protein localization during cell cycle progression by immunofluorescence. Normal human fibroblasts (WI-38) were arrested in G0 (quiescence) by serum deprivation and then stimulated by 10% serum to progress synchronously through G1 and S phase. Alternatively, we arrested cells at the G1/S boundary by stimulating G0 cells in the presence of HU; after removing HU, cells progressed synchronously through S, G2, M, and into the next cell cycle (Lu et al., 1989). We followed the fraction of cells in S by a 1-h pulse with [^{3}H]thymidine and autoradiography (% LN), and the cell cycle distribution by flow cytometry (not shown).

The BLM antibody has been characterized (Ishov et al., 1999; Neff et al., 1999; Zhong et al., 1999). As expected, it failed to stain BS fibroblasts (Fig. 1, a and b), but identified 10–30 nuclear foci in WI-38 fibroblasts (Fig. 1, d–k), confirming its specificity. To semiquantitatively assess BLM foci, we scored the fraction of WI-38 cells with >10 discernible foci per nucleus (Fig. 1 c). Quiescent cells had faint diffuse nuclear staining (not shown), but ~10% had >10 faint foci (Fig. 1 c). This staining pattern persisted as cells progressed through G1 (Q,8; Fig. 1 c). However, as cells progressed through S (after release from HU), the number (Fig. 1 c) and intensity (not shown) of BLM foci rose, increasing until most cells were in late S or G2 (HU,8; Fig. 1 c). At this time, half the cells had >10 (generally 20–40) bright BLM foci, which declined as cells entered the next cell cycle (HU,10; Fig. 1 c). The intensity and number of BLM foci were always heterogeneous, possibly due to the unavoidable loss of tight synchrony or the dynamic nature of the foci. We did not detect BLM in nucleoli, as reported for some cells (Yankiwski et al., 2000).

In sharp contrast to BLM foci, PML NBs, identified by a PML antibody, did not vary in number (10–30 per nucleus) or staining intensity, whether cells were in G0 or late S/G2 (Fig. 1, d–k). Similar results (invariant PML staining) were obtained when G0 cells were compared with cells in G1 or early S (not shown).

Although most (60–90%) PML NBs stained for BLM during late S/G2, many were devoid of BLM at other cell cycle stages. By contrast, most (80–90%) BLM foci stained for PML, regardless of cell cycle position. The few BLM foci that apparently lacked PML may indicate rare BLM localization outside PML NBs, or failure of the antibody to recognize PML in all NBs. Whatever the case, the majority of BLM colocalized with PML in human HCA2

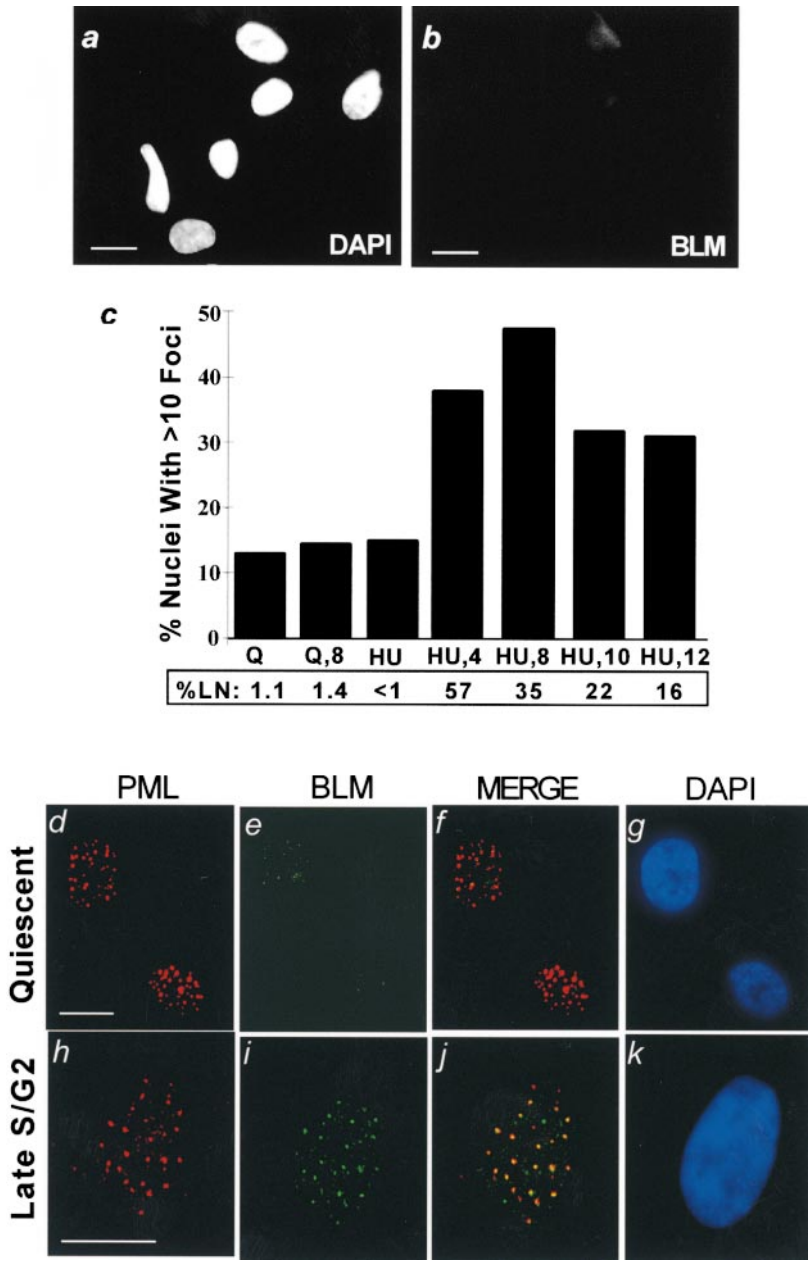

Figure 1. Cell cycle–dependent localization of BLM. Cells were synchronized, immunostained for BLM or PML, stained for nuclear DNA (DAPI), and pulsed (1 h) with [^{3}H]thymidine to determine the percentage of cells in S phase (% LN), as described in Materials and Methods. (a and b) BLM antibody specificity. Proliferating BS fibroblasts (HG2654, shown; GM11492F, not shown) were stained with DAPI (a) to visualize nuclei and the anti-BLM antibody (b). (c) BLM foci during the cell cycle. WI-38 cells were arrested in G0 (Q) and then stimulated with serum for 8 h (Q,8) to enrich for cells in mid-G1. Alternatively, cells were arrested at the G1/S boundary (HU) and released for varying intervals to enrich for cells in mid-S (HU,4), late S/G2 (HU,8), G2/M/early G1 (HU,10), or G1/early S (HU,12). The percent of LN was determined in parallel cultures. Nuclei (≥200 per data point) were scored for the presence of >10 BLM foci. (d–k) BLM and PML were identified by immunostaining using fluorescein isothiocyanate (green) or Texas red secondary antibodies. Red and green fluorescent images were superimposed (MERGE). Nuclei were identified by DAPI staining. (d) PML localization in quiescent cells. (e) BLM localization in quiescent cells. (f) Merged image of PML and BLM localization in quiescent cells. (g) DAPI staining of nuclei in d–f. (h) PML localization in cells in late S/G2. (i) BLM localization in cells in late S/G2. (j) Merged image of PML and BLM localization in cells in late S/G2. (k) DAPI staining of nuclei in h–k. Bars, ~10 μm.

normal fibroblasts, HT1080 fibrosarcoma, SAOS osteosarcoma, and VA-13 SV40-transformed fibroblasts (not shown). The exception was NB4 cells, which express a dominant negative form of PML and show abnormal PML organization into small aggregates or microspeckles (de The et al., 1991; Mu et al., 1994). As reported by Zhong et al. (1999), BLM showed mostly diffuse staining in NB4 nuclei (see Fig. 7 r), suggesting that PML is important, if not essential, for BLM focus formation.

These results indicate that PML NBs are present throughout the cell cycle, whereas BLM associates with these structures as it is expressed, predominantly during S and G2.

BLM is related to *RECQ*, which functions in HR (Harmon and Kowalczykowski, 1998), a process that provides a mechanism for repairing DNA during late S and G2 (Thompson and Schild, 1999). Thus, the BLM/PML foci that form in late S/G2 might participate in HR to repair spontaneous DNA damage that must be resolved before mitosis. Therefore, we asked whether PML NBs also contained hRAD51 or RP-A. These proteins interact, and are critical for HR and HR repair (Baumann and West, 1997; Golub et al., 1998; Kanaar et al., 1998; Thompson and Schild, 1999). Moreover, BLM was recently shown to be capable of interacting with RP-A (Brosh et al., 2000).

In quiescent cells, hRAD51 immunostaining was largely diffuse throughout the nucleus, but ~30% of nuclei contained hRAD51 foci (Fig. 2 a), 70–80% of which localized to PML NBs (Fig. 2, a–d). As cells approached late S/G2, hRAD51 staining intensity increased, and ~40% of nuclei had >10 distinct RAD51/PML foci. More than half the RAD51 foci also contained BLM (Fig. 2, e–h), and, in about a third of the cells, 80–90% of the BLM foci contained hRAD51. Western blotting showed that hRAD51 was detectable in quiescent cells, but expression increased about fivefold as cells approached late S/G2 (not shown).

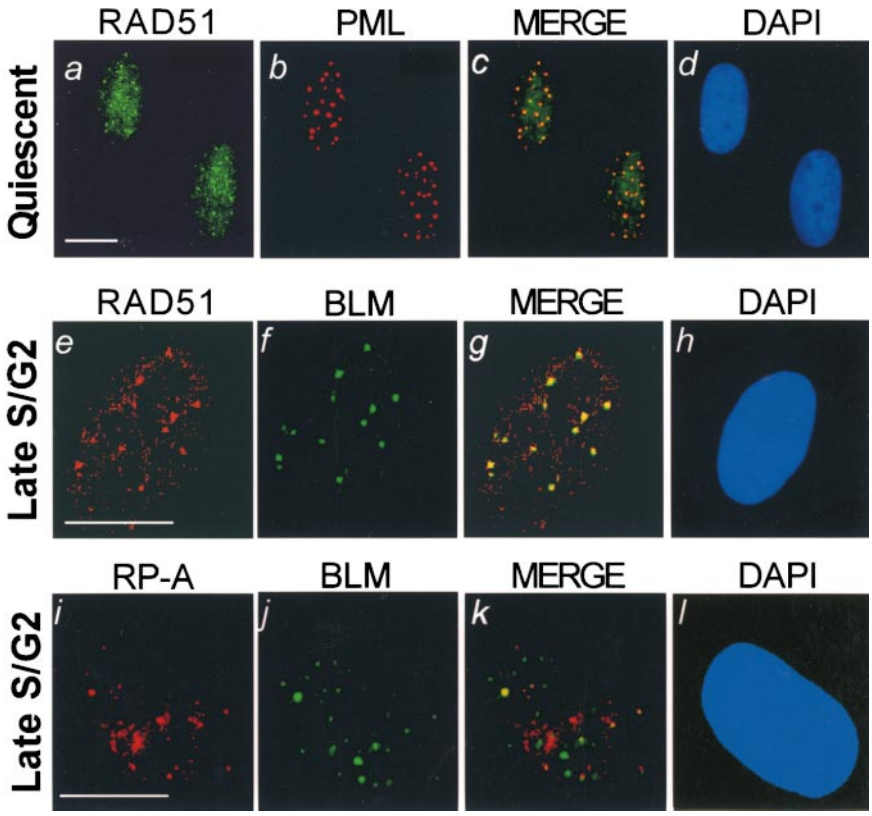

Figure 2. BLM, PML, hRAD51, and RP-A localization in cells in G0 or late S/G2. WI-38 cells were made quiescent (Quiescent), or released from a G1/S arrest for 8 h (Late S/G2). Cells were stained for BLM, PML, hRAD51, or RP-A, nuclei were visualized (DAPI), and fluorescent images were superimposed (MERGE) as described in the legend to Fig. 1. (a–d) hRAD51 and PML localization in quiescent cells. (e–h) hRAD51 and BLM localization in cells in late S/G2. (i–l) RP-A and BLM localization in cells in late S/G2. Bars, ~10 μm.

Thus, as cells progressed through late S and G2, an increasing fraction assembled nuclear foci that contained PML, BLM, and hRAD51. These results are summarized in Table I. Because 40% of cells in late S/G2 had RAD51 foci, >50% of which contained BLM, and 80–90% of BLM foci in late S/G2 localized to PML NBs, we deduce that roughly 15–20% of late S/G2 nuclei contained all three proteins (PML, RAD51, RAD51).

RP-A was evident as diffuse nuclear staining in quiescent cells, showing no obvious localization with PML or BLM (not shown). However, during late S/G2 10–20% of nuclei showed RP-A staining in a fraction of PML NBs (Table I). In those nuclei with focal RP-A staining, 20–30% of BLM-positive foci also stained positive for RP-A (Fig. 2, i–l). Thus, as cells progressed through late S/G2, 10–20% had nuclei in which 20–30% of the foci contained BLM and RP-A.

The results indicate that BLM localizes to PML NBs with hRAD51, and to a lesser extent RP-A, during late S/G2.

BLM Associates with the Nuclear Matrix and hRAD51

PML resides in the nuclear matrix (Stuurman et al., 1992), which focally concentrates nuclear processes such as RNA transcription and splicing, and DNA replication and repair (Spector, 1993; Lamond and Earnshaw, 1998). It is not known whether all components of the PML NB are bound to the nuclear matrix, or whether some components are only loosely held to the matrix by PML.

To determine how BLM associates with the PML NB, we prepared nuclear matrices from proliferating WI-38 cells using either of two methods: (a) standard high-salt extraction of nuclei, or (b) extraction at lower ionic strength followed by amine modification, which avoids the potential artifact of nonspecific salt precipitation (Wan et al., 1999). Proteins in the matrix and other fractions were analyzed by Western blotting. Regardless of the preparation method, BLM was found predominantly in the nuclear matrix fraction, cofractionating with the nuclear matrix marker protein lamin B (Spector, 1993; Lamond and Earnshaw, 1998; Wan et al., 1999; Fig. 3, a and b). BLM also fractionated with the nuclear matrix in VA-13 and HT1080 tumor cells (not shown).

BLM also interacted with hRAD51 in vitro (Fig. 3, c and d), suggesting that the colocalization of BLM and hRAD51 was a direct protein–protein interaction. Purified recombinant GST (control) or GST-BLM (Fig. 3 c) bound to glu-

Table I. Nuclear Foci Formed in Synchronized Human Fibroblasts

	Percentage of nuclei with >10 foci containing:						
Cell cycle position	PML	BLM	RAD51	RP-A	PML+BLM	PML+RAD51	PML+BLM+RAD51*
G0	>95	<10	30	<1	<10	30	<1
Late S/G2	>95	>50	30–40	10–20	>50	30–40	15–20

WI-38 cells were synchronized, and the PML, BLM, hRAD51, and RP-A proteins were detected by immunofluorescence as described in Materials and Methods.
*The fraction of nuclei containing PML, BLM, and RAD51 was deduced from the degree of PML-BLM, PML-hRAD51, and BLM-hRAD51 colocalization as described in the text.

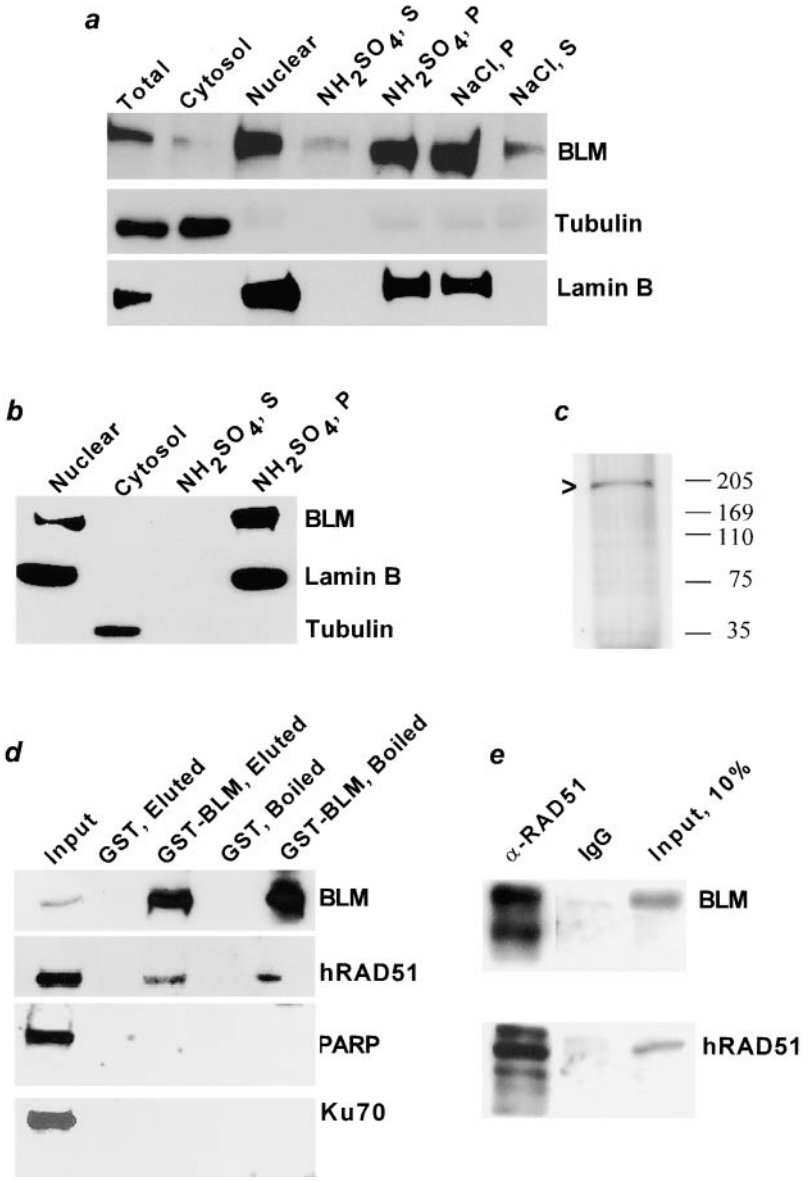

Figure 3. BLM associates with the nuclear matrix and hRAD51. Nuclear matrices were prepared from proliferating WI-38 cells by high salt extraction (NaCl), or low salt extraction and amine modification (NH_2SO_4). After extraction, 30 μg of protein was analyzed from whole cell (Total), nuclear (Nuclear), and cytoplasmic (Cytosol) lysates, and the supernatants (S) and nuclear matrix pellets (P). Proteins were analyzed for BLM, α-tubulin (Tubulin; cytosolic marker), lamin B (nuclear matrix marker), PARP, and Ku70 (DNA-associated) by Western blotting. (a–b) Results of two independent fractionations. (c) Recombinant GST-BLM. GST-BLM was produced by baculovirus in insect cells. Nuclear proteins from infected cells were bound to glutathione-Sepharose, the resin was transferred to a column, and bound proteins (200 ng) were eluted and analyzed by silver-stained SDS-PAGE. (d) hRAD51 associates with BLM. GST or GST-BLM, bound to glutathione-Sepharose beads, were incubated with SAOS-2 nuclear lysates (Input) and transferred to a column. After washing, proteins were eluted from the columns (GST, Eluted; GST-BLM, Eluted), and proteins resistant to elution were released by boiling in SDS-PAGE sample buffer (GST, Boiled; GST-BLM, Boiled). Input, eluted, and released proteins were analyzed for BLM, hRAD51, PARP, and Ku70 by Western blotting. (e) hRAD51 coimmunoprecipitates with BLM from nuclear lysates. Nuclear lysates from SOAS-2 cells (Input) were precleared and immunoprecipitated with nonspecific (IgG) or anti-hRAD51 (α-RAD51) antibody, and the immunoprecipitates were analyzed for BLM and hRAD51 by SDS-PAGE and Western blotting, as described in Materials and Methods.

tathione-Sepharose and incubated with nuclear lysates from SAOS-2 cells, which express high levels of hRAD51. The nuclear lysates were pretreated with DNase and ethidium bromide to degrade DNA and disrupt protein–DNA interactions. Proteins retained on the Sepharose were eluted with glutathione and analyzed by Western blotting. GST-BLM, but not GST, retained 30–40% of the hRAD51 in the lysate (Fig. 3 d). By contrast, neither PARP nor Ku70, nuclear DNA repair proteins that bind DNA, were retained by GST or GST-BLM (Fig. 3 d). The lack of association of PARP or Ku70, and resistance of the interaction between hRAD51 and GST-BLM to DNase or ethidium bromide, suggest that the interaction is not mediated by DNA. BLM and hRAD51 could also be coimmunoprecipitated from nuclear lysates by an anti-RAD51 antibody (Fig. 3 e). Despite this apparent interaction between BLM and hRAD51 in cell nuclei, we could not reliably coimmunoprecipitate BLM and hRAD51 using an anti-BLM antibody. This failure may be due to disruption of the BLM–hRAD51 complex by the anti-BLM antibody. Nonetheless, our immunolocalization and biochemical data suggest that BLM interacts with hRAD51, although whether this is the case in cells is not yet conclusive.

Together, the immunofluorescence and biochemical results suggest that BLM may be a component of a dynamic nuclear matrix–based complex that resides in the PML NB and may participate in HR DNA repair during G2.

BLM Increases in Response to DNA Damage

To explore the idea that BLM plays a role in DNA repair, we exposed proliferating cells to IR (5 Gy x-ray). IR causes single and double strand DNA breaks, engaging both the G1 and G2 checkpoints in normal human cells, resulting in G1 and G2 transient cell cycle arrests or delays (Kaufmann and Kies, 1998).

BLM mRNA was quantified using real-time RT-PCR (Heid et al., 1996) and QM as a constitutively expressed control mRNA (Dimri et al., 1996). IR induced a modest, transient rise in BLM mRNA, amounting to a fourfold increase within 2 h, before returning to the unirradiated (control) level (Fig. 4 a). BLM protein also increased 2–4 h after IR,

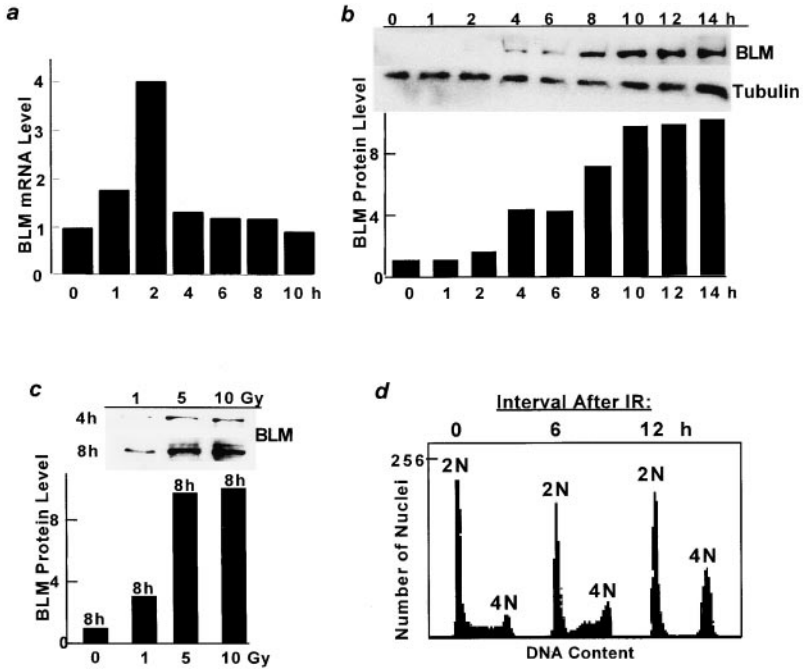

Figure 4. BLM responds to IR. Proliferating WI-38 cells were X-irradiated (IR) with 5 Gy (a, b, and d) or 0–10 Gy (c). RNA and protein were isolated, or cells were harvested for flow cytometry, at the indicated intervals (h) thereafter. *BLM* mRNA was measured by quantitative PCR using *QM* as a control; BLM protein was assessed by Western blotting using α-tubulin (Tubulin) as a control. A value of one was assigned to the normalized levels of BLM mRNA and protein in unirradiated cells (0 h). Autoradiograms of the Western analyses are shown above the histograms. (a) *BLM* mRNA after IR. (b) BLM protein after IR. (c) IR dose response. Cells were analyzed for BLM protein 4 h (autoradiogram) or 8 h (autoradiogram, histogram) after irradiation. (d) Cell cycle arrest after IR. Cells were analyzed for DNA content by flow cytometry. The G1 (2N) and G2 (4N) peaks are indicated and the fraction of cells in G1, S, and G2/M is given in the text.

but in contrast to the mRNA, continued to accumulate for 8–10 h, peaking at 10-fold over the control level. Peak BLM levels persisted for 4–6 h (12–14 h after IR; Fig. 4 b) before declining to the control level (24 h after IR; not shown). A lower dose (1 Gy) of IR induced less BLM (threefold over control), but a higher dose (10 Gy) did not increase BLM further (Fig. 4 c). Peak BLM induction by IR coincided with the arrest of cell proliferation, detected by flow cytometry. Unirradiated cultures maintained a cell cycle distribution typical of asynchronous populations (55% G1, 36% S, 9% G2/M; Fig. 4 d). Irradiated cultures, by contrast, accumulated cells in G1 (53%) and G2/M (42%) within 12 h, at which time fewer than 5% of cells were in S phase (Fig. 4 d). Because the cells have a finite replicative life span, even the early passage cultures used here contain 15–20% senescent cells, which have a G1 DNA content (Campisi, 1997). Thus, the fraction of irradiated cells that transiently arrested in G1 was likely <40%, whereas the fraction that arrested in G2 was likely >50%. Cells resumed proliferation 24 h after IR (not shown). These results raise the possibility that BLM is induced by DNA damage. Alternatively, because BLM is expressed predominantly in late S/G2, its accumulation after IR may reflect the accumulation of cells in G2.

BLM Response to DNA Damage Depends on a G2 Delay

To distinguish between these possibilities, we X-irradiated (5 Gy) quiescent cells, then stimulated them with serum. Under these conditions, cells remain in G1 for 24 h, without transiently arresting in G2 (Kaufmann and Kies, 1998; not shown). BLM levels did not change (Fig. 5 a). Similar results were obtained with irradiated senescent cells, which do not enter, much less arrest in, G2 (not shown). We also irradiated proliferating cells and immediately gave them caffeine, which abolishes the G2 delay (Busse et al., 1977; Tolmach et al., 1977; Schlegel and Pardee, 1986). Caffeine-treated cells showed a small (two- to threefold) transient rise in BLM, but no sustained BLM accumulation (Fig. 5 b) and little or no G2 delay. 3 h after IR, irradiated cultures had few, if any, mitotic figures, indicating failure to leave G2. By contrast, caffeine-treated irradiated cultures had half the mitotic index of unirradiated controls 3 h after IR, and two to three times the mitotic index of controls 6–12 h after IR (Fig. 5 b), indicating that many cells entered mitosis with little or no G2. Finally, we treated cells with other DNA damaging agents, only some of which cause a G2 delay. Bleomycin and etoposide cause DNA DSBs and G1 and G2 delays (Kaufmann and Kies, 1998). Bleomycin increased BLM six- to eightfold, very similar to the effects of IR (Fig. 5 c). Etoposide also increased BLM six- to eightfold, albeit with slower kinetics (Fig. 5 d), perhaps reflecting its slower action. In contrast, BLM was unchanged by UVC (1.6 J/m^2/s; Fig. 5 e) or hydrogen peroxide (550 μM; not shown), which cause predominantly base damage and single strand breaks and arrest normal cells primarily in G1 (Kaufmann and Kies, 1998). Thus, the rise in BLM after IR most likely reflected the transient G2 arrest that occurs when proliferating cells experience DSBs.

BLM Response to DNA Damage Is Independent of AT Mutated and p53

Further evidence that the G2 delay is responsible for the rise in BLM caused by IR came from cells deficient in AT mutated (*ATM*), the gene defective in AT. AT is a hereditary cancer-prone syndrome characterized by loss of the G1, but not the G2, DNA damage checkpoint. DNA DSBs cause AT cells to accumulate in G2 for an extended interval (Beamish et al., 1994). BLM protein was two- to fourfold less abundant in proliferating AT fibroblasts (strain AT-2SF; Tobias et al., 1984) compared with wild-type cells (WI-38), consistent with our observation that BLM is lower in slow growing cell strains compared with more rapidly dividing strains. Despite the low basal level, IR (5

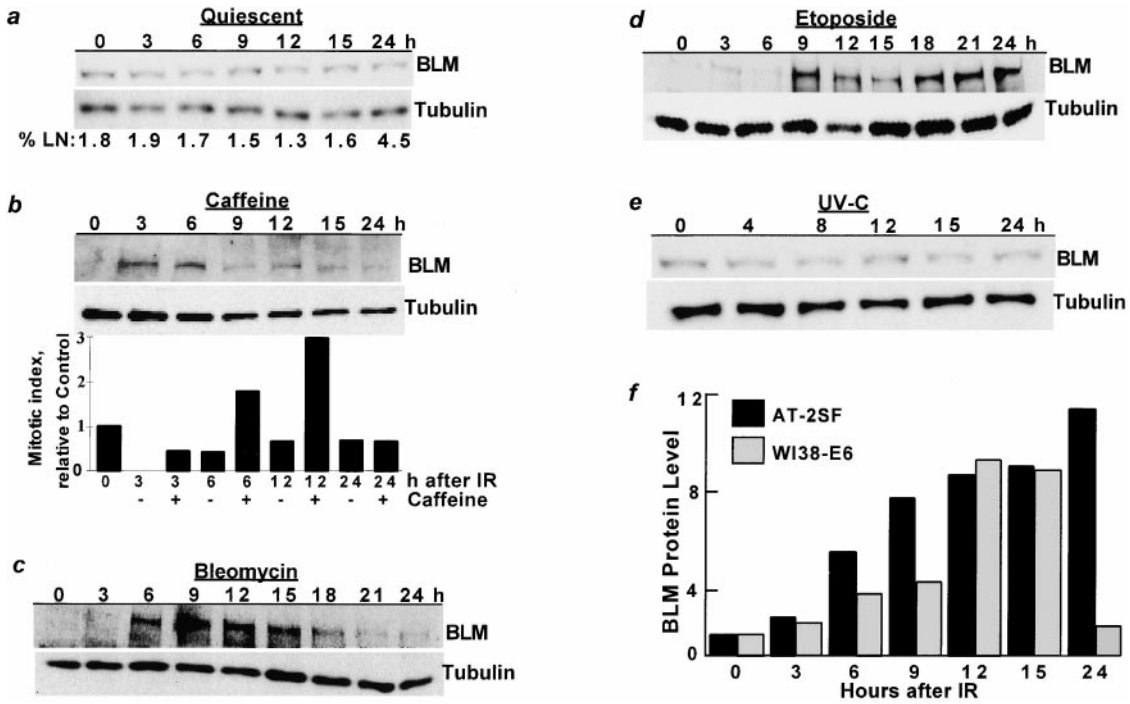

Figure 5. BLM response to DNA damage depends on the G2 delay. WI-38 (a–e), AT-2SF, or WI38-E6 (f) cells were treated with the indicated agents while quiescent (a) or proliferating (b–f). Protein lysates were prepared from untreated cells (0 h) or at the indicated times after treatment (h), and analyzed for BLM and α-tubulin (Tubulin; control) by Western blotting. (a) Quiescent cells were X-irradiated (5 Gy) and immediately stimulated with serum. Parallel cultures were pulsed for 24 h with [^{3}H]thymidine to determine the percentage of cells that synthesized DNA (% LN). (b) Proliferating cells were X-irradiated (5 Gy) and immediately given medium containing 5 mM caffeine. Parallel cultures were analyzed for mitotic figures (Mitotic index; 1,000 nuclei/point). The mitotic index of the unirradiated culture was given a value of 1. (c) Cells were given bleomycin (10 μg/ml) for 1 h in serum-containing medium. (d) Cells were given etoposide (10 μM) for 1 h in serum-containing medium. (e) Cells were irradiated with UVC (1.6 J/m^2/s) in PBS and returned to serum-containing medium. (f) Proliferating AT-2SF or WI38-E6 cells were X-irradiated (5 Gy), protein lysates were prepared, and BLM protein level was normalized to α-tubulin.

Gy x-ray) increased BLM ~10-fold in AT cells (Fig. 5 f), similar to the magnitude of increase in wild-type cells (Fig. 4 b). However, in contrast to wild-type cells, BLM remained elevated for >24 h (compared with 12–14 h for wild-type cells), consistent with their longer G2 delay.

The accumulation of BLM after IR was also independent of p53. WI-38 cells were rendered p53-deficient by expressing the E6 viral oncogene, which accelerates p53 degradation (Scheffner et al., 1990). IR (5 Gy x-ray) caused BLM accumulation (Fig. 5 f), and a transient G2 arrest (not shown), in proliferating E6-expressing cells, very similar to its effects on control cells.

BLM Foci Increase after DNA Damage

Several proteins that participate in DSB repair form nuclear foci in response to IR. These foci, known as IRIF (Maser et al., 1997), are present in undamaged cells, but increase in number after IR. One type of IRIF contains hRAD51 and RP-A, and is thought to carry out HR repair of DSBs (Haaf et al., 1995; Golub et al., 1998). Because BLM formed foci and localized with hRAD51 and RP-A in a fraction of undamaged nuclei, we asked whether BLM foci, like RAD51/RP-A IRIF, increased after IR.

BLM foci were heterogeneously distributed in asynchronous cultures, with few nuclei containing >10 foci (Fig. 6 a). However, after X-irradiation (5 Gy) nuclei with >10 BLM foci rose, whereas those with <10 foci declined, in a time- (Fig. 6 a) and dose- (not shown) dependent manner. 10 h after IR, nuclei with >10 BLM foci were four- to fivefold more prevalent than in control cultures. Moreover, at this time 15–20% of irradiated nuclei had >20 BLM foci, whereas such nuclei were rare in controls (Fig. 6 b). The IR-induced peak in BLM foci (Fig. 6 a) coincided with the IR-induced peak in BLM protein and G2 delay (Fig. 4). Etoposide similarly increased BLM foci coincident with BLM protein and a G2 delay (not shown). By contrast, BLM foci did not rise after UV irradiation (Fig. 6 b), which did not increase BLM expression (Fig. 5 e) and delays cells in G1 (Kaufmann and Kies, 1998). Compared with controls, UV-irradiated cultures had more nuclei with ≤10 BLM foci, and fewer with 11–20 BLM foci (Fig. 6 b), consistent with their more prominent G1 delay. Thus, BLM foci increased in response to agents that cause DSBs, similar to IRIF, and the increase coincided with the G2 delay.

IR increased the number of BLM foci in proliferating SV40-transformed cells (VA-13; not shown), which lack p53 function, MO59J cells (not shown), which lack the catalytic subunit of DNA-dependent protein kinase (DNA-PK), and AT-2SF cells (Fig. 6 c), which lack ATM. AT cultures accumulated two- to threefold more nuclei with >20 BLM foci than wild-type cultures 10 h after IR (Fig. 6 c), consistent with their prolonged peak of BLM expression

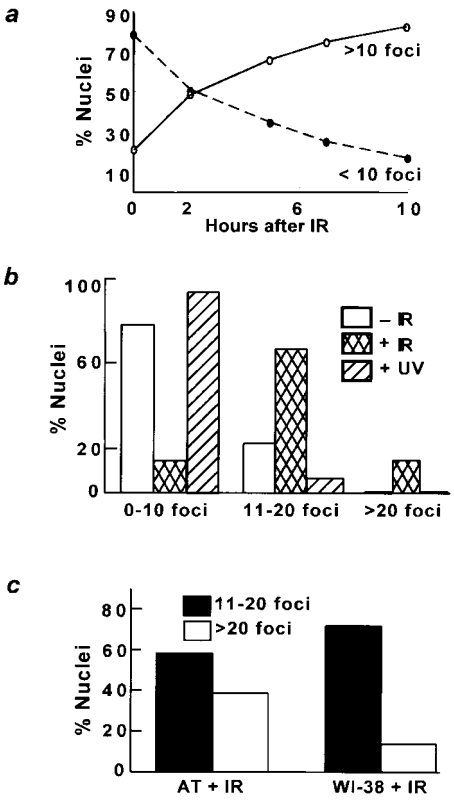

Figure 6. BLM focus formation after DNA damage. Proliferating WI-38 (a–c) and AT-2SF (c) cells were X-irradiated (5 Gy) or UV-irradiated (1.6 J/m^2/s) and immunostained for BLM at the indicated intervals thereafter. BLM foci were counted in 200 nuclei per point. (a) BLM foci increase after IR. Nuclei were scored for the presence of >10 or <10 BLM foci. (b) Effect of IR versus UV. Cells were unirradiated (−IR) or irradiated with X-rays (+IR) or UV (+UV). 10 h later, nuclei were scored for the presence of 0–10, 11–20, or >20 BLM foci. (c) BLM foci formation in irradiated AT cells. Proliferating AT-2SF or WI-38 cells were X-irradiated. 10 h later, nuclei were scored for the presence of 11–20 or >20 BLM foci.

(Fig. 5 f) and G2 delay (Beamish et al., 1994). Interestingly, AT cells also accumulate more RAD51 IRIF than wild-type cells (Maser et al., 1997).

BLM and PML Are Components of IRIF

The rise in BLM foci caused by IR and prevalence of BLM (Fig. 6 c) and hRAD51 (Maser et al., 1997) foci in irradiated AT cells suggest that BLM might be a component of RAD51 IRIF. To test this idea, we immunostained cells for BLM, hRAD51, and RP-A 10–12 h after IR, when the G2 delay, BLM expression, and BLM foci were maximal. At this time, ~50% of nuclei had >20 hRAD51 and/or RP-A foci. Greater than 90% of the RAD51 foci costained for BLM and >90% of BLM foci costained for hRAD51 (Fig. 7, a–d). Thus, there was near complete colocalization of BLM and RAD51 to the same foci after IR. RP-A foci were more numerous than BLM/RAD51 foci (>30 per nucleus; Fig. 7 f), with ~60% containing BLM; ~70% of BLM foci contained RP-A (Fig. 7, e–h). BLM remained localized to PML NBs after IR, evident by the high coincidence of BLM and PML staining (Fig. 7, i–l). These results indicate that BLM and PML are components of RAD51 IRIF and a fraction of RP-A IRIF. Because RP-A foci outnumbered BLM/RAD51 foci after IR, RP-A may function in some IR responses that are distinct from those in which BLM and hRAD51 participate, or act with different kinetics.

BLM was not essential for RAD51 IRIF formation because BS cells formed abundant RAD51 foci in response to IR (Fig. 7, m–o). BS cells formed 2–2.5-fold more RAD51 foci as normal cells, consistent with reduced or delayed repair. By contrast, few IRIF formed in NB4 cells, which express a dominant negative form of PML. In control NB4 cells, hRAD51 and BLM were largely dispersed throughout the nucleus (Fig. 7, p and r). IR induced a few hRAD51 and BLM foci, but most of the hRAD51 and BLM remained disperse (Fig. 7, q and s). This result suggests that, in contrast to BLM, PML is important for IRIF formation.

BLM Associates with Single-stranded DNA after Damage

RAD 51/RP-A IRIF are important for HR DNA repair and, after IR, accumulate at sites of single-stranded DNA (Raderschall et al., 1999) or unscheduled DNA synthesis (Haaf et al., 1999). If BLM and PML are components of RAD51 IRIF and participate in repair, they should accumulate at sites of repair. BrdU, a thymidine analogue, has been used to visualize sites of single-stranded DNA and presumptive DSB repair (Raderschall et al., 1999). BrdU is inaccessible to an anti-BrdU antibody when present in duplex DNA, but readily accessible to the antibody when the DNA is denatured or single stranded. We used BrdU to determine whether BLM/PML foci associate with single-stranded DNA after IR-induced damage.

Cells were grown for two doublings in the presence of BrdU. Proliferating BrdU-labeled cells, fixed and stained under nondenaturing conditions, showed no significant staining (Fig. 8 a), confirming that the antibody does not detect BrdU in duplex DNA. The same cells showed the expected heterogeneous pattern of BLM foci (Fig. 8 b), indicating that BrdU did not perturb BLM localization. When BrdU-labeled cells were X-irradiated (5 Gy), BrdU foci appeared (Fig. 8 c), peaking 8–10 h after IR. At this time, >50% of the cells had multiple BrdU foci. These foci were not due to apoptosis because there was no evidence of PARP degradation, which precedes apoptotic DNA fragmentation, for at least 10 h after IR (Fig. 8 d). Moreover, BrdU foci appeared to be a specific response to DSBs because UV induced few if any BrdU foci (not shown). Thus, in agreement with Raderschall et al. (1999), BrdU foci formed primarily in response to DNA DSBs, where they presumably identify sites of repair.

To determine whether BLM localized with BrdU, we costained for BLM and BrdU 10–12 h after IR. A significant fraction of BLM localized to BrdU foci. In 30–50% of cells with BrdU foci, 80–90% of the BrdU foci costained for BLM and 80–90% of the BLM foci in these cells costained for BrdU (Fig. 8, e–g). In the remaining cells with BrdU foci, BLM was present in a variable fraction of BrdU foci, ranging from 30 to 50% (Fig. 8, h–m). Moreover, PML also associated with a significant fraction of BrdU foci (Fig. 8, n–p). Thus, in response to IR, BLM and PML NBs, like RAD51 and RP-A (Raderschall et al.,

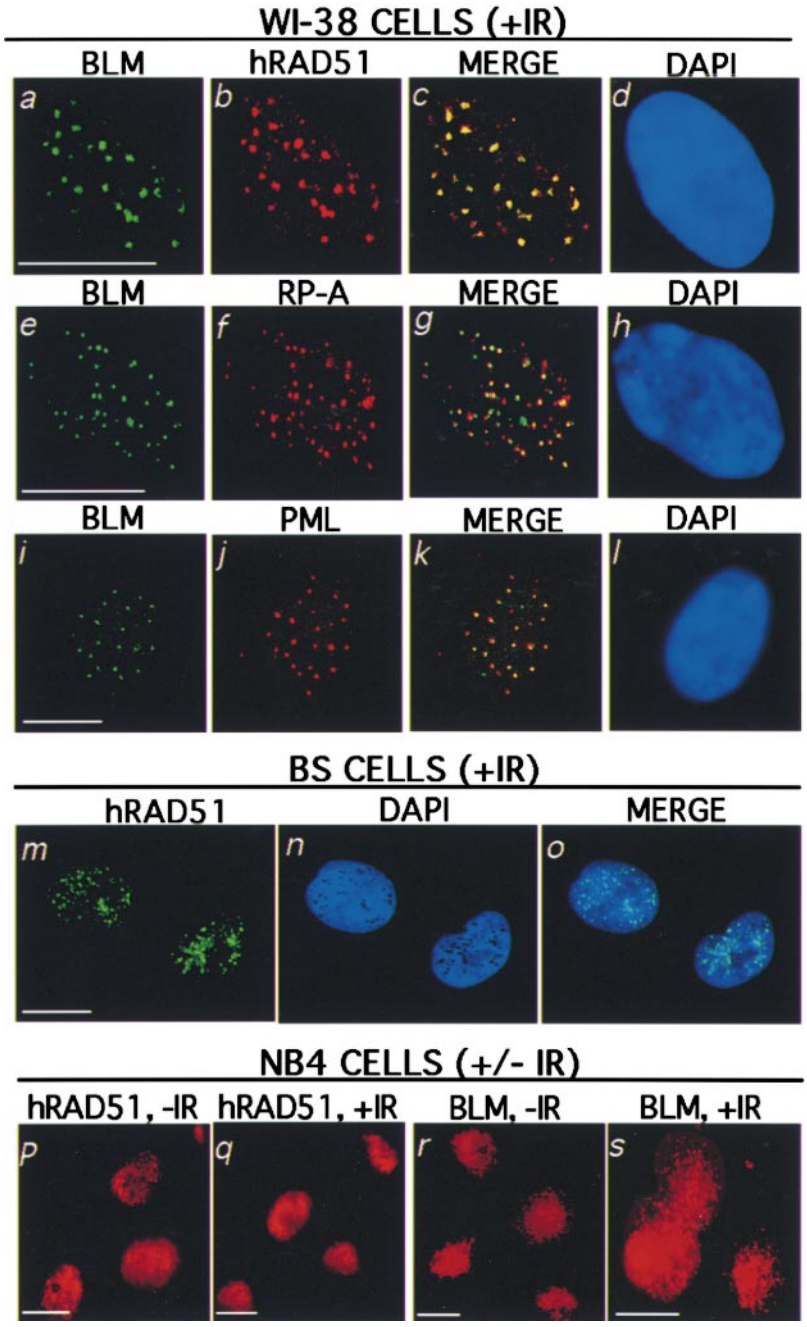

Figure 7. BLM localizes with hRAD51, RP-A, and PML after IR. Proliferating WI-38, BS HG2654, and NB4 cells were X-irradiated (5 Gy) where indicated. 10 h after irradiation, the cells were immunostained for BLM, PML, hRAD51, or RP-A; nuclei were visualized (DAPI); and fluorescent images were superimposed (MERGE) as described in the legend to Fig. 1. (a–d) BLM and hRAD51 localization in irradiated WI-38 cells. (e–h) BLM and RP-A localization in irradiated WI-38 cells. (i–l) BLM and PML localization in irradiated WI-38 cells. (m–o) hRAD51 localization in irradiated BS cells. (p–s) hRAD51 and BLM localization in unirradiated (−IR) and irradiated (+IR) NB4 cells. Bars, ~10 μm.

1999), assembled at sites of single-stranded DNA, which presumably are undergoing HR repair.

Discussion

Defects in BLM have severe physiological consequences in humans, the most prominent of which is premature death due to cancer. At the cellular level, defects in BLM cause genomic instability, particularly chromosome aberrations and SCEs. The phenotypes associated with BLM deficiency, and the homology to RECQ, suggest that BLM may function in an HR DNA repair pathway that resolves spontaneous and induced DNA damage. In support of this idea, we confirmed that BLM is expressed primarily in late S/G2, when HR repair is operational, and found it was induced by agents that cause DNA DSBs and engage the G2 checkpoint. We also found that BLM is a component of RAD51 IRIF, which are thought to be important for the repair of DSBs by HR. Our data suggest that BLM and RAD51 interact, and BLM was found to interact with RP-A (Brosh et al., 2000). BLM foci contained RAD51, and to a lesser extent RP-A, and formed in undamaged cells during G2. BLM foci containing RAD51 also formed in IR-damaged cells, where they localized to sites of presumptive repair. During the cell cycle and after IR, the majority of BLM associated with PML NBs, a matrix-based organizing center for many nuclear processes. PML appeared to be important for organizing BLM and hRAD51 into foci, particularly IRIF. Together, our results suggest that BLM participates in normal G2 functions and the G2

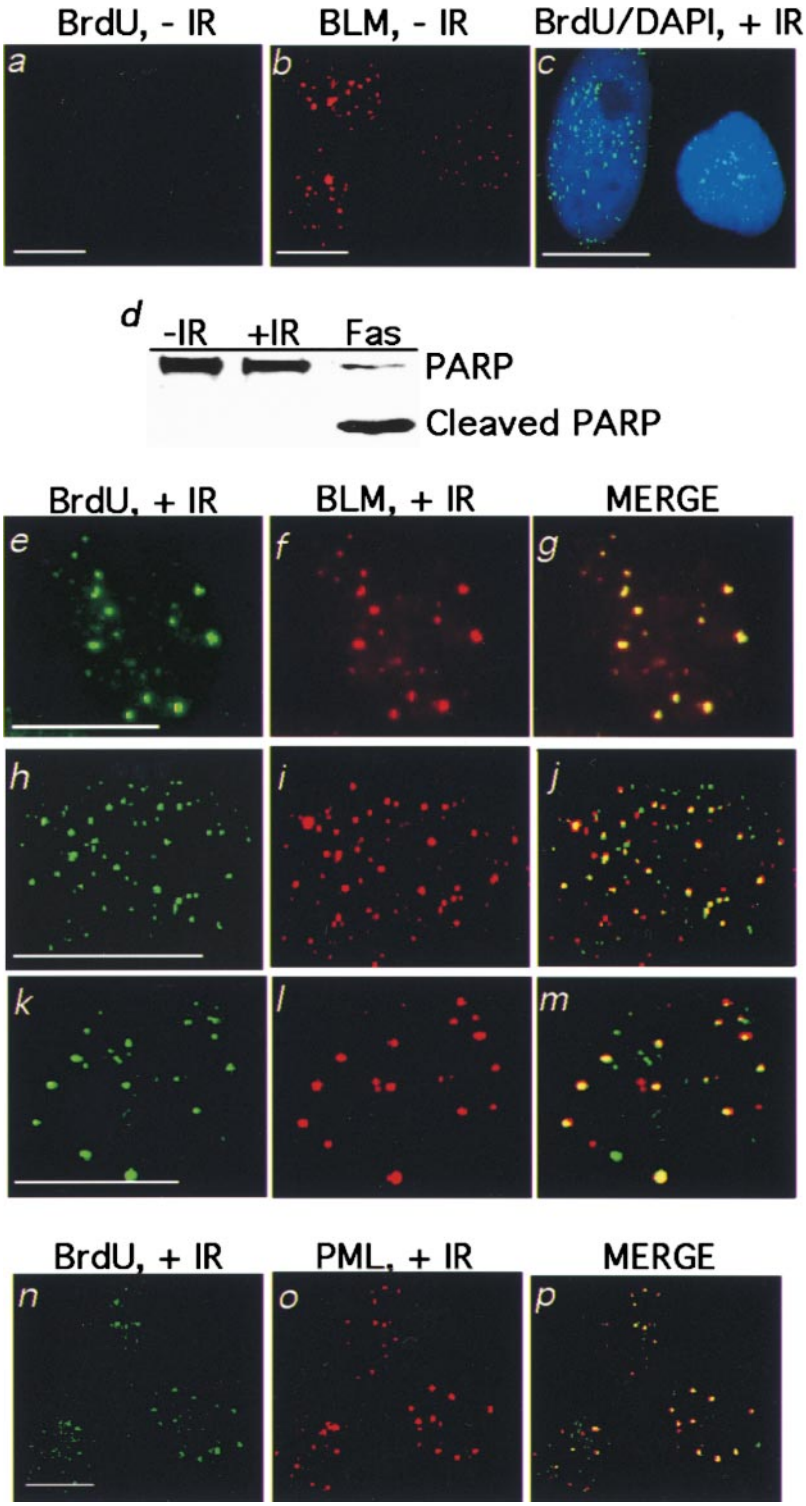

Figure 8. BLM and PML localize to sites of putative DNA repair after IR. Proliferating WI-38 were labeled for two doublings with BrdU and X-irradiated (5 Gy) where indicated. 10–12 h after irradiation, the cells were fixed under nondenaturing conditions and immunostained for BrdU, BLM, and PML. Nuclei were visualized (DAPI) and fluorescent images were superimposed (MERGE) as described in the legend to Fig. 1. (a) BrdU staining in unirradiated cells. (b) BLM foci in unirradiated, BrdU-labeled cells. (c) BrdU and DAPI staining in irradiated cells. The BrdU and DAPI images were merged. (d) PARP integrity after irradiation. BrdU-labeled cells were left untreated (−IR), X-irradiated (+IR), or treated with Fas ligand (Fas; positive control for apoptosis). 10 h later, protein lysates were prepared and analyzed for PARP by Western blotting. (e–m) BLM and BrdU localization in irradiated cells. e–g show a cell with 80–90% colocalization of BLM and BrdU foci; 30–50% of cells with BrdU foci showed this staining pattern. h–m show cells in which BLM and BrdU colocalized to varying degrees. (n–p) PML and BrdU localization in irradiated cells. Bar, ~10 μm.

DNA damage response, and implicates the PML NB in assembling BLM, hRAD51, and probably other proteins that are important for both processes.

Function in Undamaged Cells

BLM foci formed predominantly in late S and G2 and increased during the G2 delay induced by DNA DSB, suggesting that BLM participates in a G2 function. In undamaged cells, BLM may be needed for proper termination of DNA replication. As the genome is duplicated, excessive recombination must be suppressed and sister chromatids must be disentangled to ensure accurate mitosis. Consistent with this idea, BS cells accumulate replication intermediates (Ockey and Saffhill, 1986; Lonn et al., 1990). BLM may also regulate mitotic recombination during G2. SCEs are mediated by hRAD51 and hRAD54 and can repair DNA lesions by HR at the end of S phase (Sonoda et al., 1999). Whether BLM stimulates or suppresses recom-

bination is not yet known. BLM may suppress recombination during normal cell cycle progression, but promote recombination during repair of DSBs. BLM also localizes with RP-A (Walpita et al., 1999) and RAD51 (Moens et al., 2000) in mammalian spermatocytes undergoing meiotic prophase (Walpita et al., 1999). This localization and the male infertility characteristic of BS suggest that BLM may also function during meiosis.

Response to DNA Damage and Role in HR DNA Repair

BS cells have been reported to be more sensitive than wild-type cells to radiation, particularly in late S and G2 (Aurias et al., 1985; Hall et al., 1986). BLM protein increased and assembled into foci specifically in response to agents that caused DNA DSBs. This induction and assembly was not a primary response to DSBs. Rather, it reflected engagement of the G2 checkpoint and the arrest of cells in G2. DNA DSBs are potentially catastrophic lesions because they can lead to unequal distribution of DNA to daughter cells. Mammalian cells are thought to repair DNA DSBs primarily by nonhomologous end joining (Karanjawala et al., 1999), but recent evidence shows that HR is also important for resolving such damage (Kanaar et al., 1998; Thompson and Schild, 1999). Repair by HR requires extensive regions of sequence homology, which are provided by the undamaged sister chromatid. Hence, HR repair occurs almost exclusively in S or G2. HR repair is carried out by the RAD52 complex, which includes hRAD51 and RP-A (Kanaar et al., 1998; Thompson and Schild, 1999). Several lines of evidence suggest that BLM participates in HR repair: (a) BLM is most highly expressed in late S and G2, when HR occurs; (b) BLM interacted with hRAD51, which is critical for HR; (c) BLM colocalized with hRAD51, and to a lesser extent RP-A (also important for HR), in both undamaged and damaged cells; (d) many of the RAD51 foci that formed after IR contained BLM; and (e) BLM foci localized to sites of presumptive repair (single-stranded DNA) after IR.

BLM IRIF were more prevalent in AT cells, relative to wild-type cells. AT cells are known to accumulate fewer RAD50/MRE11 IRIF and more RAD51 IRIF than wild-type cells (Maser et al., 1997). The RAD50–MRE11 complex, with proteins like DNA-PK, participates in DSB repair by nonhomologous end joining. *ATM*, the gene defective in AT, encodes a kinase that phosphorylates p53 in response to IR, increasing its half-life and affinity for target genes (Banin et al., 1998; Canman et al., 1998). Because p53 activation is impaired, AT cells do not undergo a G1 checkpoint arrest, but rather enter a prolonged G2 delay after IR (Beamish et al., 1994). This delay coincided with a prolonged period of elevated BLM and BLM IRIF. Because RAD50/MRE11 foci are deficient in damaged AT cells and BLM/RAD51 foci persist, DSBs normally repaired by nonhomologous end joining may be repaired by HR in AT cells. Our finding that BLM IRIF form independent of ATM, p53, and DNA-PK are consistent with the idea that BLM IRIF participate in HR repair.

Our findings do not rule out additional roles for BLM, for example in other DNA repair pathways. The recent finding that BLM is a component of a supercomplex containing the RAD50–MRE11 complex and proteins important for transcription-coupled repair (Wang et al., 2000) suggests that BLM may participate in multiple DNA transactions.

Role of PML NBs

PML may play an important role in assembling BLM/hRAD51 foci during normal G2 progression and during the G2 delay induced by IR. Regardless of cell cycle position or DNA damage, the majority of BLM localized to PML NBs. In undamaged cells, some BLM/PML NBs also contained hRAD51. However, after irradiation the majority of BLM/PML foci contained hRAD51, and a substantial fraction of these foci also contained RP-A. Thus, IRIF contained BLM and PML, in addition to RAD51 and RP-A. This was not the case in NB4 cells, in which PML is dysfunctional. In undamaged NB4 cells, neither BLM nor hRAD51 was organized into foci. Rather, both proteins were dispersed throughout the nucleus. After NB4 cells were irradiated, neither BLM nor RAD51 IRIF foci formed. Thus, PML appears to be essential for the formation of IRIF. By contrast, BLM does not appear to be essential for PML NB formation (Ishov et al., 1999; Zhong et al., 1999). Likewise, BLM did not appear to be required for RAD51 IRIF formation, since BS cells formed RAD51 foci in response to IR.

PML NBs appear to be sites of BLM, RAD51, and RP-A assembly during late S/G2, and after irradiation. Both BLM and PML localized to sites of single-stranded DNA and presumptive repair after damage by IR. Thus, one function of PML NBs may be to assemble RAD51/BLM IRIF to carry out HR DNA repair during S/G2 in undamaged cells and during G2 in damaged cells. It is also possible that PML NBs are involved in assembling RAD50/MRE11 IRIF, but this remains to be determined.

In the absence of PML function, the NB structure is disrupted and cells either arrest growth or undergo apoptosis (de The et al., 1991; Mu et al., 1994; Le et al., 1996; Wang et al., 1998a,b). One possibility is that these cellular responses are due to a failure to resolve DNA damage at the end of S phase or during G2. The association of BLM and PML with the nuclear matrix and with IRIF and sites of presumptive DSB repair suggest that PML NBs assemble a matrix-based complex containing BLM and hRAD51 which functions as a HR recombinosome to repair spontaneous and induced DNA DSBs.

We thank Drs. E. Blakely, J. German, O. Pereira-Smith, and D. Chen for cell lines, and D. Chen for antibodies and helpful discussions.

Supported by grants from the National Institute on Aging (AG11658) to J. Campisi under Department of Energy contract DE-AC0376SF00098 to the University of California, and by the Sloan-Kettering Institute and May Samual Rudin Family Foundation to N.A. Ellis.

Submitted: 1 May 2000
Revised: 6 February 2001
Accepted: 20 February 2001

References

Aurias, A., J.L. Antoine, R. Assathiany, M. Odievre, and B. Dutrillaux. 1985. Radiation sensitivity of Bloom's syndrome lymphocytes during S and G2 phases. *Cancer Genet. Cytogenet.* 16:131–136.

Banin, S., L. Moyal, S. Shieh, Y. Taya, C.W. Anderson, L. Chessa, N.I. Smorodinsky, C. Prives, Y. Reiss, Y. Shiloh, and Y. Ziv. 1998. Enhanced phosphorylation of p53 by ATM in response to DNA damage. *Science.* 281:1674–1677.

Baumann, P., and S.C. West. 1997. The human Rad51 protein: polarity of strand transfer and stimulation by hRP-A. *EMBO (Eur. Mol. Biol. Organ.)*

J. 16:5198–5206.
Beamish, H., K.K. Khanna, and M.F. Lavin. 1994. Ionizing radiation and cell cycle progression in ataxia telangiectasia. *Radiat. Res.* 138:130–133.
Brosh, R.M., J.L. Li, M.K. Kenny, J.K. Karow, M.P. Cooper, R.P. Kureekattil, I.D. Hickson, and V.A. Bohr. 2000. Replication protein A physically interacts with the Bloom's syndrome protein and stimulates its helicase activity. *J. Biol. Chem.* 275:23500–23508.
Busse, P.M., S.K. Bose, R.W. Jones, and L.J. Tolmach. 1977. The action of caffeine on X-irradiated HeLa cells. II. Synergistic lethality. *Radiat. Res.* 71: 666–677.
Campisi, J. 1997. The biology of replicative senescence. *Eur. J. Cancer.* 33:703–709.
Canman, C.E., D.S. Lim, K.A. Cimprich, Y. Taya, K. Tamai, K. Sakaguchi, E. Appella, M.B. Kastan, and J.D. Sciliano. 1998. Activation of the ATM kinase by ionizing radiation and phosphorylation of p53. *Science.* 281:1677–1679.
Compton, D.A., T. Yen, and D.W. Cleveland. 1991. Identification of a novel centromere/kinetochore-associated protein using monoclonal antibodies generated against human mitotic chromosome scaffolds. *J. Cell Biol.* 112: 1083–1097.
Davey, S., C.S. Han, S.A. Ramer, J.C. Klassen, A. Jacobson, A. Eisenberger, K.M. Hopkins, H.B. Lieberman, and G.A. Freyer. 1998. Fission yeast rad121 regulates cell cycle checkpoint control and is homologous to the Bloom's syndrome disease gene. *Mol. Cell. Biol.* 18:2721–2728.
de The, H., C. Lavau, A. Marchio, C. Chomienne, L. Degos, and A. Dejean. 1991. The PML-RAR alpha fusion mRNA generated by the t(15;17) translocation in acute promyelocytic leukemia encodes a functionally altered RAR. *Cell.* 66:675–684.
Dignam, J.D., R.M. Lebovitz, and R.G. Roeder. 1983. Accurate transcription initiation by RNA polymerase II in a soluble extract from isolated mammalian nuclei. *Nucleic Acids Res.* 11:1475–1489.
Dimri, G.P., E.E. Hara, and J. Campisi. 1994. Regulation of two E2F-related genes in presenescent and senescent human fibroblasts. *J. Biol. Chem.* 269: 16180–16186.
Dimri, G.P., X. Lee, G. Basile, M. Acosta, G. Scott, C. Roskelley, E.E. Medrano, M. Linskens, I. Rubelj, O.M. Pereira-Smith, M. Peacocke, and J. Campisi. 1995. A novel biomarker identifies senescent human cells in culture and in aging skin in vivo. *Proc. Natl. Acad. Sci. USA.* 92:9363–9367.
Dimri, G.P., A. Testori, M. Acosta, and J. Campisi. 1996. Replicative senescence, aging and growth regulatory transcription factors. *Biol. Signals.* 5:154–162.
Dimri, G.P., K. Itahana, M. Acosta, and J. Campisi. 2000. Regulation of a senescence checkpoint response by the E2F1 transcription factor and p14/ ARF tumor suppressor. *Mol. Cell. Biol.* 20:273–285.
Dutertre, S., M. Ababou, R. Onclercq, J. Delic, B. Chatton, C. Jaulin, and M. Amor-Gueret. 2000. Cell cycle regulation of the endogenous wild type Bloom's syndrome DNA helicase. *Oncogene.* 19:2731–2738.
Ellis, N.A., and J. German. 1996. Molecular genetics of Bloom's syndrome. *Hum. Mol. Genet.* 5:1457–1463.
Ellis, N.A., J. Groden, T.Z. Ye, J. Straughen, D.J. Lennon, S. Ciocci, M. Proytcheva, and J. German. 1995. The Bloom's syndrome gene product is homologous to RecQ helicases. *Cell.* 83:655–666.
Fukuchi, K., G.M. Martin, and R.J. Monnat. 1989. Mutator phenotype of Werner syndrome is characterized by extensive deletions. *Proc. Natl. Acad. Sci. USA.* 86:5893–5897.
German, J. 1993. Bloom syndrome: a Mendelian prototype of somatic mutational disease. *Medicine*. 72:393–406.
Gharibyan, V., and H. Youssoufian. 1999. Localization of the Bloom syndrome helicase to punctate nuclear structures and the nuclear matrix and regulation during the cell cycle: comparison with the Werner's syndrome helicase. *Mol. Carcinog.* 26:261–273.
Golub, E.I., R.C. Gupta, T. Haaf, M.S. Wold, and C.M. Radding. 1998. Interaction of human hRAD51 recombination protein with single-stranded DNA binding protein, RPA. *Nucleic Acids Res.* 26:5388–5393.
Goto, M. 1997. Hierarchical deterioration of body systems in Werner's syndrome: implications for normal ageing. *Mech. Ageing Dev.* 98:239–254.
Gray, M.D., J.C. Shen, A.S. Kamath-Loeb, A. Blank, B.L. Sopher, G.M. Martin, J. Oshima, and L.A. Loeb. 1997. The Werner syndrome protein is a DNA helicase. *Nat. Genet.* 17:100–103.
Gray, M.D., L. Wang, H. Youssoufian, G.M. Martin, and J. Oshima. 1998. Werner helicase is localized to transcriptionally active nucleoli of cycling cells. *Exp. Cell Res.* 242:487–494.
Haaf, T., E.I. Golub, G. Reddy, C.M. Radding, and D.C. Ward. 1995. Nuclear foci of mammalian HRAD51 recombination protein in somatic cells after DNA damage and its localization in synaptonemal complexes. *Proc. Natl. Acad. Sci. USA*. 92:2298–2302.
Haaf, T., E. Raderschall, G. Reddy, D.C. Ward, C.M. Radding, and E.I. Golub. 1999. Sequestration of mammalian Rad51-recombination protein into micronuclei. *J. Cell Biol.* 144:11–20.
Halbert, C.L., G.W. Demes, and D.A. Galloway. 1992. The E7 gene of human papillomavirus type 16 is sufficient for immortalization of human epithelial cells. *J. Virol.* 66:2125–2134.
Hall, E.J., M.J. Marchese, M.B. Astor, and T. Morse. 1986. Response of cells of human origin, normal and malignant, to acute and low dose rate irradiation. *Int. J. Radiat. Oncol. Biol. Phys.* 12:655–659.
Hanada, K., T. Ukita, Y. Kohno, K. Saito, J. Kato, and H. Ikeda. 1997. RecQ DNA helicase is a suppressor of illegitimate recombination in *Escherichia coli*. *Proc. Natl. Acad. Sci. USA*. 94:3860–3865.
Harmon, F.G., and S.C. Kowalczykowski. 1998. RecQ helicase, in concert with RecA and SSB proteins, initiates and disrupts DNA recombination. *Genes Dev.* 12:1134–1144.
Heid, C.A., J. Stevens, K.J. Livak, and P.M. Williams. 1996. Real time quantitative PCR. *Genome Res*. 6:986–994.
Ishov, A.M., A.G. Sotnikov, D. Negorev, O.V. Vladimirova, N. Neff, T. Kamitani, E.T.H. Yeh, J.F. Strauss, and G.G. Maul. 1999. PML is critical for ND10 formation and recruits the PML-interacting protein Daxx to this nuclear structure when modified by SUMO-1. *J. Cell Biol.* 147:221–233.
Kanaar, R., J.H. Hoeijmakers, and D.C. van Gent. 1998. Molecular mechanisms of DNA double strand break repair. *Trends Cell Biol.* 12:483–489.
Karanjawala, Z.E., U. Grawunder, C.L. Hsieh, and M. Lieber. 1999. The nonhomologous DNA end joining pathway is important for chromosome stability in primary fibroblasts. *Curr. Biol.* 9:1501–1504.
Karow, J.K., R.K. Chakraverty, and I.D. Hickson. 1997. The Bloom's syndrome gene product is a 3′-5′ DNA helicase. *J. Biol. Chem.* 272:30611–30614.
Kaufmann, W.K., and P.E. Kies. 1998. DNA signals for G2 checkpoint response in diploid human fibroblast. *Mutat. Res.* 400:153–167.
Kitao, S., I. Ohsugi, K. Ichikawa, M. Goto, Y. Furuichi, and A. Shimamoto. 1998. Cloning of two new human helicase genes of the RecQ family: biological significance of multiple species in higher eukaryotes. *Genomics.* 54:443–452.
Lamond, A.I., and W.C. Earnshaw. 1998. Structure and function in the nucleus. *Science*. 280:547–553.
Le, X.F., P. Yang, and K.S. Chang. 1996. Analysis of the growth and transformation suppressor domains of promyelocytic leukemia gene, PML. *J. Biol. Chem.* 271:130–135.
Lonn, U., S. Lonn, U. Nylen, G. Winblad, and J. German. 1990. An abnormal profile of DNA replication intermediates in Bloom's syndrome. *Cancer Res.* 50:3141–3145.
Lu, K.H., R.A. Levine, and J. Campisi. 1989. c-ras-Ha gene expression is regulated by insulin or insulinlike growth factor and by epidermal growth factor in murine fibroblasts. *Mol. Cell. Biol.* 9:3411–3417.
Martin, G.M., J. Oshima, M.D. Gray, and M. Poot. 1999. What geriatricians should know about the Werner syndrome. *J. Am. Geriatr. Soc.* 47:1136–1144.
Maser, R.S., K.J. Monsen, B.E. Nelms, and J.H. Petrini. 1997. hMre11 and hRad50 nuclear foci are induced during the normal cellular response to DNA double-strand breaks. *Mol. Cell. Biol.* 17:6087–6096.
Miozzo, M., P. Castorina, P. Riva, L. Dalpra, A.M. Fuhrman Conti, L. Volpi, T.S. Hoe, A. Khoo, J. Wiegant, C. Rosenberg, and L. Larizza. 1998. Chromosomal instability in fibroblasts and tumors from 2 sibs with Rothmund-Thomson syndrome. *Int. J. Cancer.* 77:504–510.
Moens, P.B., R. Freire, M. Tarsounas, B. Spyropoulos, and S.P. Jackson. 2000. Expression and nuclear localization of BLM, a chromosome stability protein mutated in Bloom's syndrome, suggest a role in recombination during meiotic prophase. *J. Cell Sci.* 113:663–672.
Mu, Z.M., K.V. Chin, J.H. Liu, G. Lozano, and K.S. Chang. 1994. PML, a growth suppressor disrupted in acute promyelocytic leukemia. *Mol. Cell. Biol.* 14:6858–6867.
Neff, N.F., N.A. Ellis, T.Z. Ye, J. Noonan, K. Huang, M. Sanz, and M. Proytcheva. 1999. The DNA helicase activity of BLM is necessary for the correction of the genomic instability of Bloom syndrome cells. *Mol. Biol. Cell.* 10:665–676.
Ockey, C.H., and R. Saffhill. 1986. Delayed DNA maturation, a possible cause of the elevated sister-chromatid exchange in Bloom's syndrome. *Carcinogenesis*. 7:53–57.
Pucillo, C., S. Salzano, S. Pepe, M. Vitale, S. Formisano, and G. Rossi. 1990. Regulation of the expression of the low-affinity IgE receptor (Fc epsilon RII) in the human monocyte-like cell line U-937 by phorbol esters and IgE. *Int. Arch. Allergy Appl. Immunol.* 93:330–337.
Puranam, K.L., and P.J. Blackshear. 1994. Cloning and characterization of RECQL, a potential human homologue of the *Escherichia coli* DNA helicase RecQ. *J. Biol. Chem*. 269:29838–29845.
Raderschall, E., E.I. Golub, and T. Haaf. 1999. Nuclear foci of mammalian recombination proteins are located at single-stranded DNA regions formed after DNA damage. *Proc. Natl. Acad. Sci. USA*. 96:1921–1926.
Scheffner, M., B.A. Werness, J.M. Huibregtse, A.J. Levine, and P.M. Howley. 1990. The E6 oncoprotein encoded by human papillomavirus types 16 and 18 promotes the degradation of p53. *Cell*. 63:1129–1136.
Schlegel, R., and A.B. Pardee. 1986. Caffeine-induced uncoupling of mitosis from the completion of DNA replication in mammalian cells. *Science*. 232: 1264–1266.
Seki, M., H. Miyazawa, S. Tada, J. Yanagisawa, T. Yamaoka, S. Hoshino, K. Ozawa, T. Eki, M. Nogami, K. Okumura, et al. 1994. Molecular cloning of cDNA encoding human DNA helicase Q1 which has homology to *Escherichia coli* Rec Q helicase and localization of the gene at chromosome 12p12. *Nucleic Acids Res*. 22:4566–4573.
Sonoda, E., M.O. Sasaki, C. Morrison, Y. Yamaguchi-Iwal, M. Takata, and S. Takeda. 1999. Sister-chromatid exchanges are mediated by homologous recombination in vertebrate cells. *Mol. Cell. Biol*. 19:5166–5169.
Spector, D.L. 1993. Macromolecular domains in the cell nucleus. *Annu. Rev. Cell Biol*. 9:265–315.
Starr, D.G., J.P. McClure, and J.M. Connor. 1985. Non-dermatological compli-

cations and genetic aspects of the Rothmund-Thomson syndrome. *Clin. Genet*. 27:102–104.

Stewart, E., C.R. Chapman, F. Al-Khodairy, A.M. Carr, and T. Enoch. 1997. Rqh11, a fission yeast gene related to the Bloom's and Werner's syndrome genes, is required for reversible S phase arrest. *EMBO (Eur. Mol. Biol. Organ.) J*. 16:2682–2692.

Stuurman, N., A. de Graaf, A. Floore, A. Josso, B. Humbel, L. de Jong, and R. van Driel. 1992. A monoclonal antibody recognizing nuclear matrix-associated nuclear bodies. *J. Cell Sci*. 101:773–784.

Tada, S., J. Yanagisawa, T. Sonoyama, A. Miyajima, M. Seki, M. Ui, and T. Enomoto. 1996. Characterization of the properties of a human homologue of *Escherichia coli* RecQ from xeroderma pigmentosum group C and from HeLa cells. *Cell Struct. Funct.* 21:123–132.

Thompson, L.H., and D. Schild. 1999. The contribution of homologous recombination in preserving genome integrity in mammalian cells. *Biochimie*. 81: 87–105.

Tobias, C.A., E.A. Blakely, P.Y. Chang, L. Lommel, and R. Roots. 1984. Response of sensitive human ataxia and resistant T-1 cell lines to accelerated heavy ions. *Br. J. Cancer*. 6:175–185.

Tolmach, L.J., R.W. Jones, and P.M. Busse. 1977. The action of caffeine on X-irradiated HeLa cells. I. Delayed inhibition of DNA synthesis. *Radiat. Res*. 71:653–665.

Vennos, E.M., and W.D. James. 1995. Rothmund-Thomson syndrome. *Dermatol. Clin*. 13:143–150.

Walpita, D., A.W. Plug, N.F. Neff, J. German, and T. Ashley. 1999. Bloom's syndrome protein, BLM, colocalizes with replication protein A in meiotic prophase nuclei of mammalian spermatocytes. *Proc. Natl. Acad. Sci. USA*. 96:5622–5627.

Wan, K.M., J.A. Nickerson, G. Krockmalnic, and S. Penman. 1999. The nuclear matrix prepared by amine modification. *Proc. Natl. Acad. Sci. USA*. 96:933–938.

Wang, Y., D. Cortez, P. Yazdi, N. Neff, S.J. Elledge, and J. Qin. 2000. BASC, a super complex of BRCA1-associated proteins involved in the recognition and repair of aberrant DNA structures. *Genes Dev*. 14:927–939.

Wang, Z., D. Ruggero, S. Ronchetti, M. Zhong, M. Gaboli, R. Rivi, and P. Pandolfi. 1998a. PML is essential for multiple apoptotic pathways. *Nat. Genet*. 20:266–272.

Wang, Z.G., L. Delva, M. Gaboli, R. Rivi, M. Giorgio, C. Cordon-Cardo, F. Grosveld, and P. Pandolfi. 1998b. Role of PML in cell growth and the retinoic acid pathway. *Science*. 279:1547–1551.

Watt, P.M., and I.D. Hickson. 1996. Failure to unwind causes cancer. Genome stability. *Curr. Biol*. 6:265–267.

Watt, P.M., I.D. Hickson, R.H. Borts, and E.J. Louis. 1997. SGS1, a homologue of the Bloom's and Werner's syndrome genes, is required for maintenance of genome stability in *Saccharomyces cerevisiae*. *Genetics*. 144:935–945.

Wessel, G.M., and D.R. McClay. 1986. Two embryonic, tissue-specific molecules identified by a double-label immunofluorescence technique for monoclonal antibodies. *J. Histochem. Cytochem*. 34:703–706.

Yankiwski, V., R.A. Marciniak, L. Guarente, and N.F. Neff. 2000. Nuclear structure in normal and Bloom syndrome cells. *Proc. Natl. Acad. Sci. USA*. 97:5214–5219.

Yu, C.E., J. Oshima, Y.H. Fu, E.M. Wijsman, F. Hisama, R. Alisch, S. Matthews, J. Nakura, T. Miki, S. Ouais, et al. 1996. Positional cloning of the Werner's syndrome gene. *Science*. 272:258–262.

Zhong, S., P. Hu, T.Z. Ye, R. Stan, N.A. Ellis, and P.P. Pandolfi. 1999. A role for PML and the nuclear body in genomic stability. *Oncogene*. 18:7841–7847.